ANALYSIS OF TRANSONIC AERODYNAMIC INTERFERENCE IN THE WING-NACELLE REGION FOR A GENERIC TRANSPORT AIRCRAFT

Ante Soda and Ralph Voss

DLR Institute of Aeroelasticity, Bunsenstrasse 10, D-37073 Göttingen, Germany
e-mail: ante.soda@dlr.de

Keywords: Unsteady transonic aerodynamics, wing-nacelle interference, shock-buffet

Abstract: This paper presents results of a numerical investigation dealing with steady and unsteady aerodynamic wing-nacelle-pylon (WNP) interference effects. In the first part of the paper the design process of the generic WIONA (Wing with Oscillating Nacelle) geometry is described. It is shown that development of major interference effects in the channel between wing and nacelle strongly depends on geometrical parameters of the configuration. After the geometry definition, the steady viscous interference effects are investigated and the influence of different flow parameters is analysed. It is shown that viscous interference features are dominated by the interaction between shock wave and boundary layer. In the last part of the paper an analysis is given of the unsteady aerodynamics features characteristic for a WNP cluster. The unsteady aerodynamic response to the pitching oscillations is investigated and it is shown that local flow separation and re-attachment play a crucial role in the possible aerodynamic excitation of the structure. Additionally, the issue of self-sustained shock oscillation occurring in the WNP region in the case of stationary geometry (shock-buffet) is investigated.

1 INTRODUCTION

Flight tests and wind tunnel experiment data for modern transport aircraft configurations with large wing-span show that an unsteady channel-type transonic flow in the region of wing, nacelle and pylon (Figure 1) may induce structural vibrations [1,2]. In the early 1990s, an experimental study of interference effects [1] indicated a significant effect of the wing/nacelle interference effect on flutter critical speed. Unfortunately, the detailed aerodynamic data from that campaign is not available since the aeroelastic effects were of major concern and the flow field in the WNP region was not of primary interest. Taking into account the continuous trend of increasing engine nacelle diameters and the related aeroelastic safety issues, a detailed numerical and experimental investigation of unsteady transonic aerodynamic interference effects occurring in the WNP region has been initiated between DLR and ONERA (project WIONA). Objectives of the investigation are:

- to numerically and experimentally investigate unsteady interference effects in the WNP region (including possible shock-buffet oscillations) and the effects from a spinning engine fan,
- to obtain data relevant for validation of CFD tools for prediction of complex unsteady phenomena.

Wind tunnel testing is performed in the transonic wind tunnel in Göttingen (TWG), Germany, with both partners, DLR and ONERA, sharing the work of wind tunnel model development, manufacturing, measurements and validation of simulation codes. The current paper gives an overview of the DLR computational work in the WIONA project.

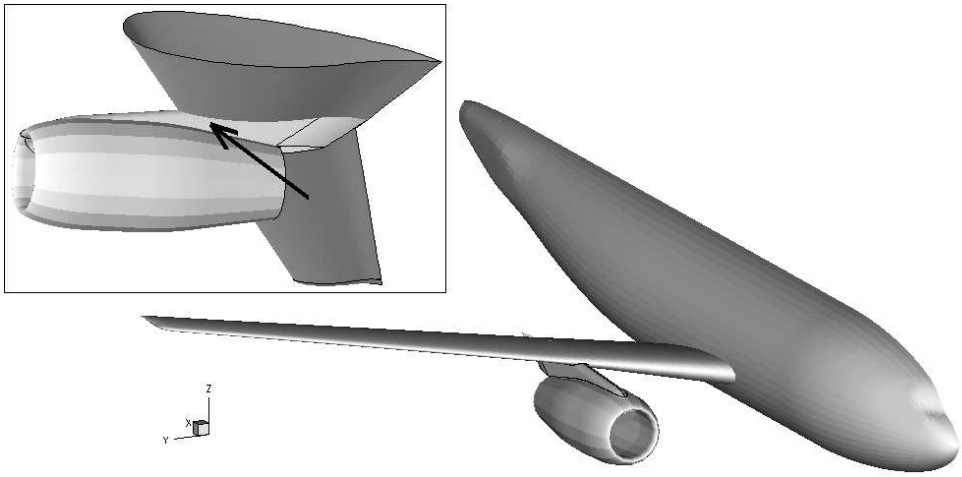

Figure 1: Acceleration of the flow in the region between wing, pylon and nacelle (channel effect) can introduce unsteady aerodynamic effects and give rise to aeroelastic issues.

2 NUMERICAL TOOLS

Steady and unsteady calculations presented in the paper are made by two CFD codes based on different numerical approaches. For the viscous and inviscid flow field simulations on unstructured/hybrid grids the DLR-Tau solver [3] is used. It is a time-accurate Reynolds-averaged Navier-Stokes (URANS) code based on a finite-volume approach for spatial discretization, an explicit multi-step Runge-Kutta scheme for inner-iterations and implicit dual time-stepping for temporal discretization. In order to accelerate the convergence to a steady state, local time stepping, residual smoothing and a multigrid technique based on agglomeration of the dual-grid volumes are used. Two eddy-viscosity turbulence models are employed for the Navier-Stokes calculations with the Tau code: the 1-equation model of Spalart and Allmaras [3] and the linearised explicit algebraic stress model based on the 2-equation k-ω proposal of Wilcox [3]. For the spatial gradients of flow fluxes, both upwind and central differencing schemes can be employed. The second solver used in the investigation is an Euler viscous-inviscid multi-block structured code, EUVIMB [4], developed at the DLR Institute of Aeroelasticity. This solver uses a centered scheme corrected with the second and fourth order artificial dissipation terms and an explicit multi-stage Runge-Kutta scheme for the time integration. The EUVIMB code is used for the inviscid flow simulations on multi-block grids in the design phase of the WIONA model.

With respect to the computational grids, an in-house developed 3-D grid generator Aengus MB [4] is used to generate structured multi-block body-fitted grids for the inviscid flow simulations with the structured CFD code. All the grid blocks are of 'H' topological type and a typical Euler grid contains about 0.9 million cells in total (Figure 2 left). A commercial grid generation software Centaur [5] is used to generate unstructured and hybrid grids for calculations with the Tau code. The Tau code Euler calculations are performed with the pure unstructured grids consisting typically of 0.35 million nodes and about 2 million computational cells, while a grid with 2 (6) million nodes (cells) is used for the N-S simulations (Figure 2 right).

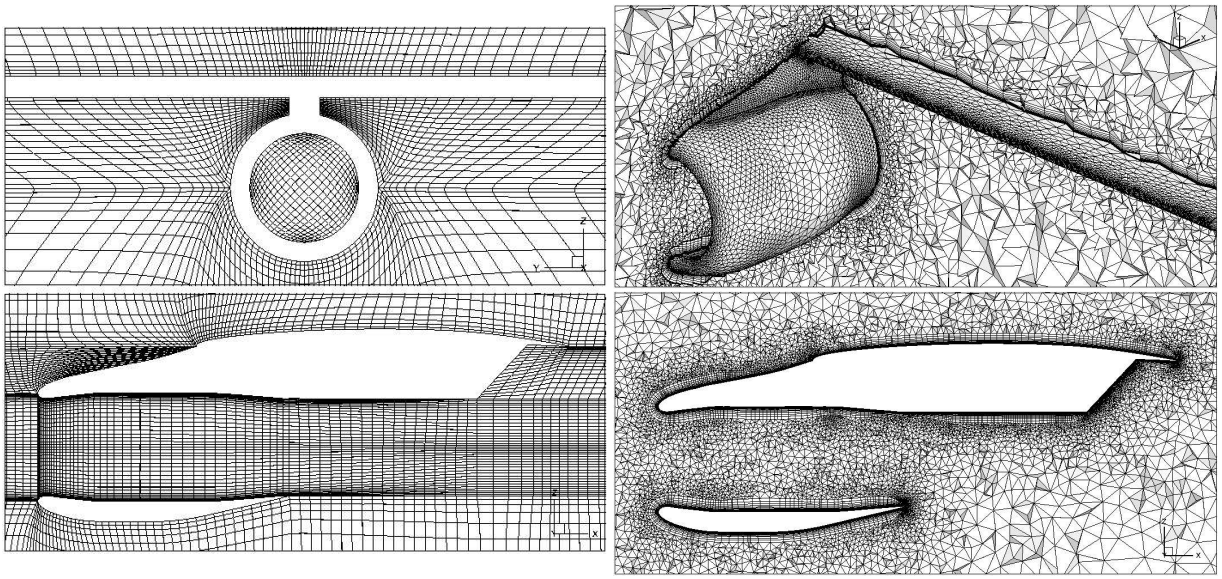

Figure 2: Structured (left) and hybrid (right) computational grids used in the study.

3 WIONA GEOMETRY

The geometry of the WNP configuration used in the project (WIONA geometry) is chosen such to closely resemble the WNP clusters employed on realistic Airbus passenger aircrafts. The WIONA model is a generic assembly of two different geometries. For the wing entity a HPF7 supercritical aerofoil (derived from the Airbus A340 aerofoil) is used, while the geometry of WIONA nacelle-pylon cluster is based on the nacelle from the generic DLR-F6 configuration [6]. The geometry of the wind-tunnel WIONA model is defined using the inviscid steady computational analysis [4], under consideration of wind-tunnel and production constraints. Due to the restrictions of excitationa mechanism in the TWG wind tunnel [7], a wall-to-wall wing section has to be chosen and an excitation system applied on both W-T walls. Further restriction is the inability to achieve realistic wing sweep so the model has to be designed with the smaller sweep angle.

In the WIONA design phase two Euler CFD codes are used in order to investigate the influence of following geometrical parameters: wing sweep angle, wing/nacelle overlapping, nacelle yaw angle and pylon thickness. The results show that, due to a channel effect in the WNP region, strong flow acceleration exists on the wing lower surface. As a result, a supersonic region occurs which is closed by a relatively strong shock wave (Figure 3, left), depending on the wing-nacelle overlap (dx parameter, see Figure 3, right). Flow on the upper surface of the wing, in contrast, is only slightly affected by the channel effect. Furthermore, it is shown that the development and the strength of WNP interference effects strongly depends on the nacelle yaw angle (Figure 3, right). The influence of wing sweep angle, on the other hand, is only of secondary importance and its effects on the aerodynamic interaction in the channel flow can be replaced by the influence of nacelle yaw angle (compare pressure distributions on the right side of Figure 3). Thus, the interference effects of a swept-wing/nacelle configuration can be simulated by a rectangular wing and a nacelle yawing degree of freedom. Based on these findings the configuration with zero wing sweep angle, $dx = 0.25$*chord, and the nacelle with the variable yaw angle is chosen as the WIONA model for the wind-tunnel measurements (Figure 4).

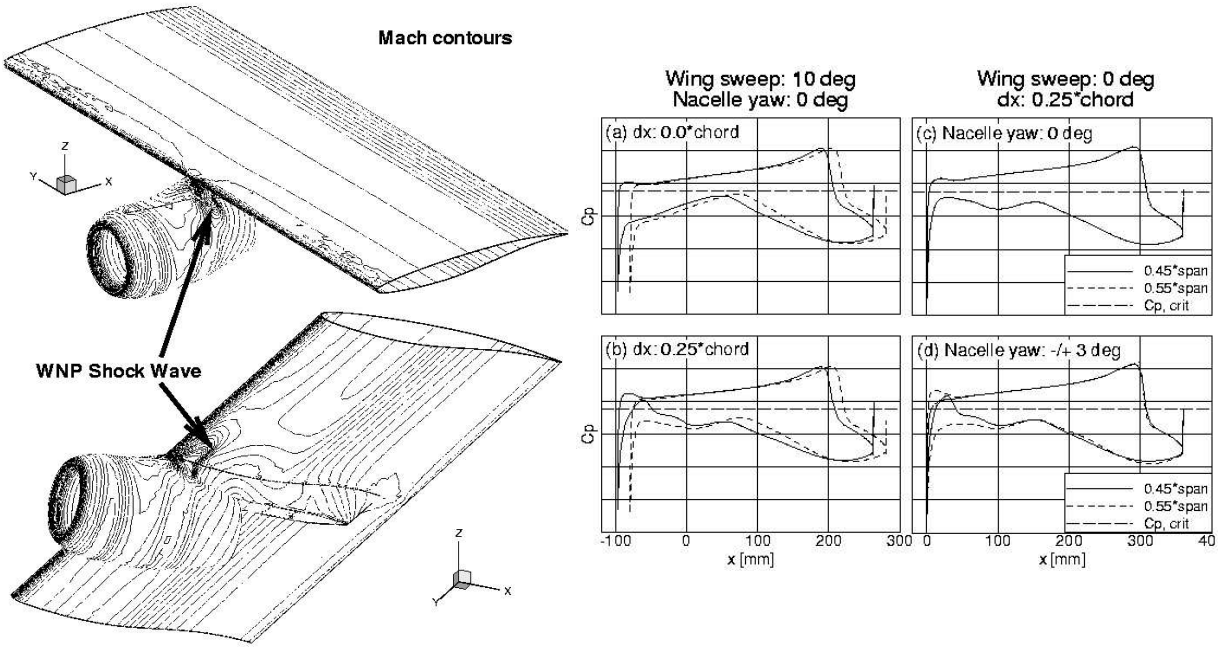

Figure 3: Results of inviscid calculations with the Tau code. Left: Mach number distribution on surface of the WIONA model. Right: influence of variation of geometric parameters.

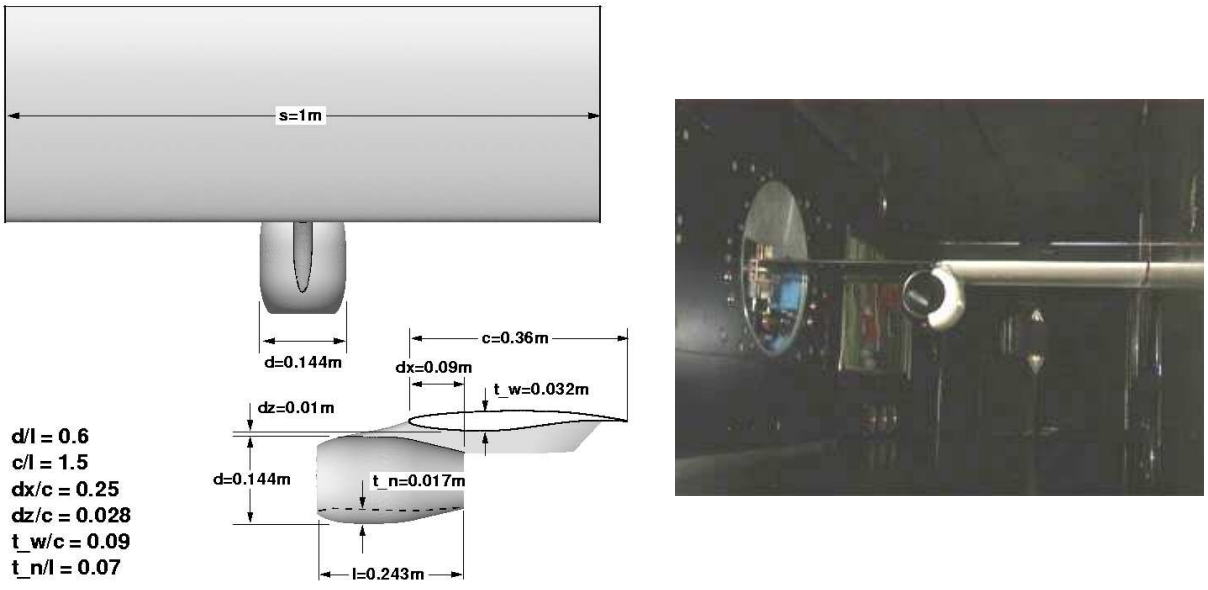

Figure 4: Final WIONA geometry. Left: dimensions of the model. Right: wind-tunnel model with 136 pressure tappings in 4 sections.

4 STEADY VISCOUS INTERFERENCE EFFECTS

Following the geometry definition, a detailed investigation of the steady viscous interference effects has been performed, using the variation of flow parameters (Mach number and incidence angle) and modeling parameters (different turbulence models and spatial discretisation schemes for flow fluxes). The basic test case for the viscous simulations has the following flow parameters: $Ma = 0.82$, $Re = 2.2$ million, incidence $\alpha = -0.6$ deg. Figure 5 shows that numerical results obtained with three different combinations of turbulence models and solver schemes are in good agreement with the wind tunnel data [7] for the following measurement point: $Ma = 0.826$ and $\alpha = 0.09$ deg. The experimental integral lift and moment coefficients achieved with these parameters are the same as coefficients calculated for the above basic test case. Both turbulence models returned very similar results, the only difference being a slightly larger WNP suction peak predicted by the 1-equation model (Figures 5c and 5d).

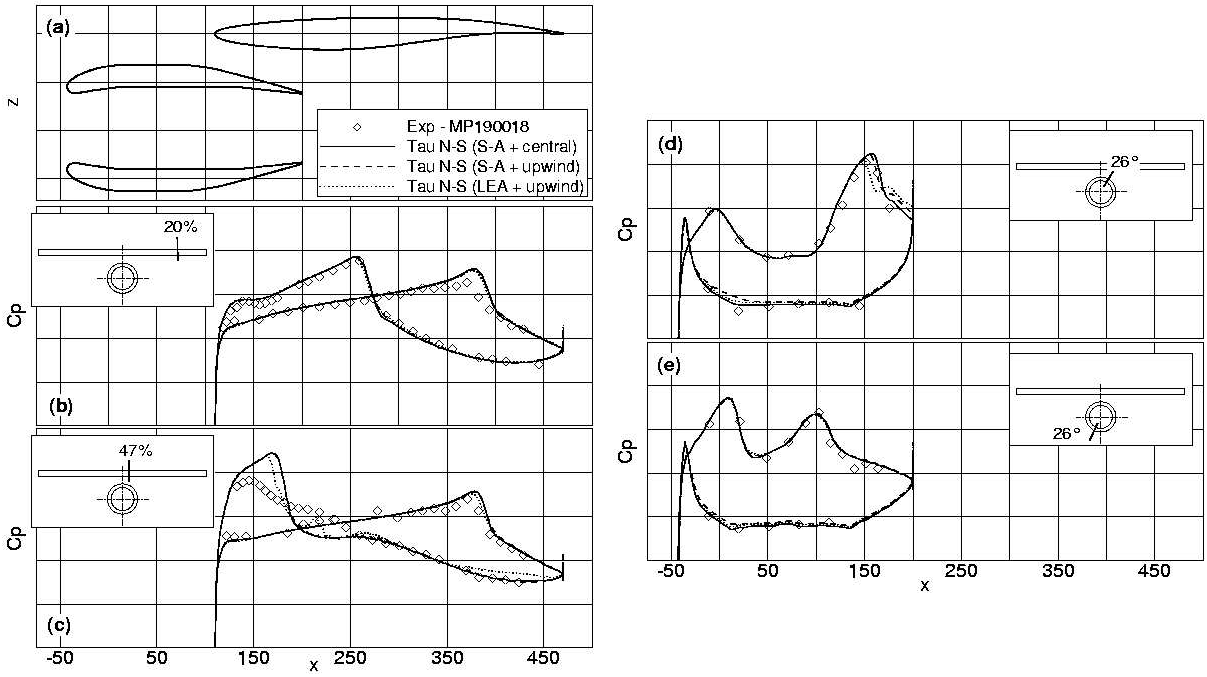

Figure 5: Comparison of calculated and experimental pressure distributions at four spanwise sections. Numerical results obtained with different combinations of modelling parameters.

With respect to the validation of calculated results, the only discrepancy from the measured data is the numerical over-prediction of the strength of interference shock (too large numerical suction peak) on the wing lower surface (cut-plane at 47% span, Figure 5c). Interestingly, the same shock occurring on the upper part of the nacelle in the WNP region was captured perfectly by all three combinations of modelling parameters (Figure 5d). Two interesting supersonic regions occurring on the surface of the model are the region in WNP channel (Figures 5c, 5d and 6a) and the region on wing upper surface (Figures 5a and 6a), both of them terminated by shock waves. In the WNP region the normal shock is spanning the channel and on both walls of the channel (upper and lower) the fanning of the normal shock can be seen (double λ-shock system, Figure 6c). On both sides the pressure rise accross the upstream shock is much larger than accross the downstream foot, feature typical for the interaction between shock wave and turbulent boundary layer [4,8]. The

weaker (downstream) shock foot is not strong enough to slow down the flow to a subsonic regime, so a local supersonic region (tongue) extends downstream until it is terminated by recompression waves. The analysis of x-component of velocity (Figure 6b) and stream traces on the geometry surface (Figure 6d) shows that in the WNP channel, where the highest local Mach number appears, the shock is strong enough to induce separation of the boundary layer on both wing and nacelle. The existence of a supersonic tongue delays the closure of the bubble [8] and this leads to the extension of the separated flow regime all the way to the trailing edge of nacelle. On the wing lower surface the separation bubble manages to re-attach immediately after the flow below it becomes subsonic (downstream of a supersonic tongue). The strong adverse pressure gradient on the wing lower surface, however, manages to provoke a second separation close to the trailing edge (Figure 6b). On the wing upper surface the shock induces a significant increase of the boundary layer thickness but for this test case the flow remains attached. Additional small supersonic regions on the lower half of nacelle (Figure 5e and Figure 6a) are not typical for realistic engine nacelles and appear on the WIONA model because the nacelle profile had to be thick enough to accomodate the pressure sensors.

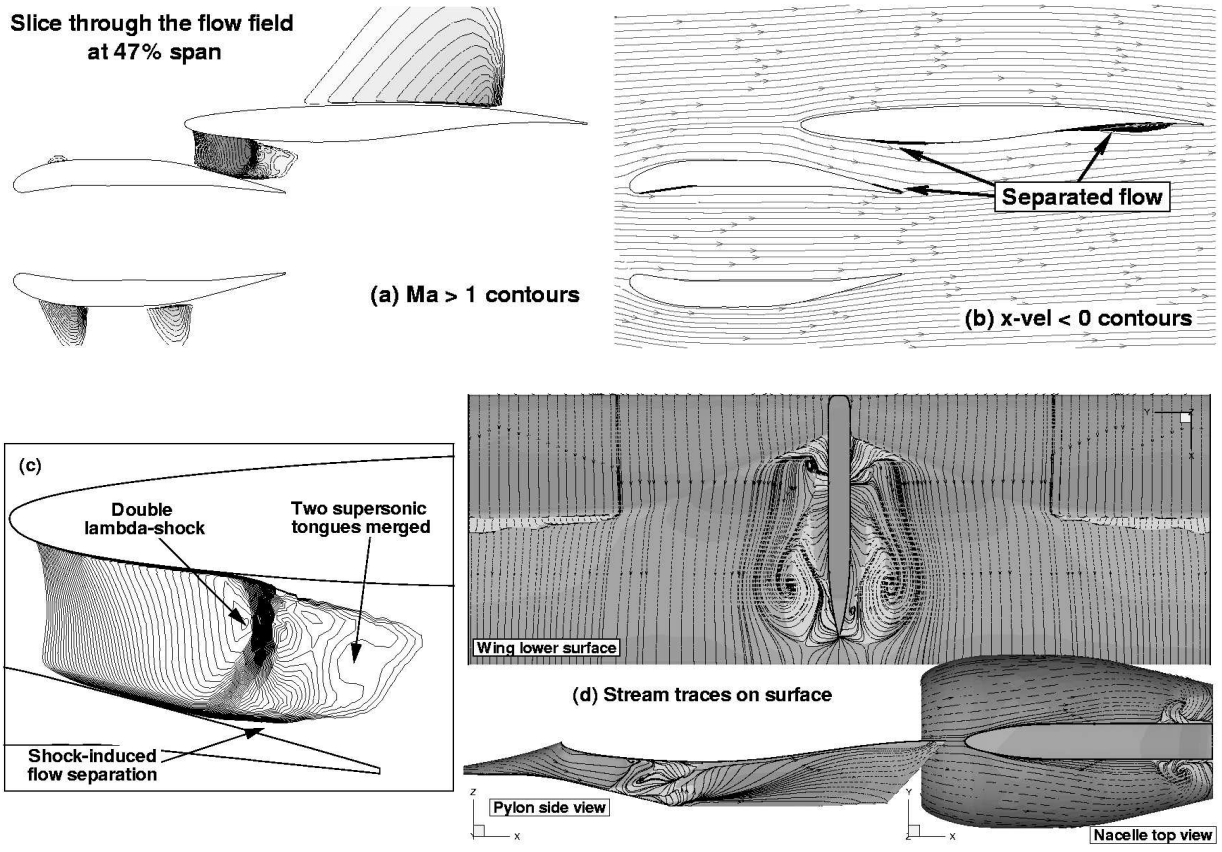

Figure 6: Steady aerodynamic phenomena in the flow field (a, b and c) and on the surface (d) of the WIONA geometry.

5 AERODYNAMIC RESPONSE TO OSCILLATING GEOMETRY

The unsteady RANS computations are performed with the TAU code for a forced pitching motion of the complete WIONA model (rigid body oscillation) around the presented steady flow condition. The unsteady flow parameters are: pitching axis at $x/c = 0.25$, pitching amplitude $\Delta\alpha_{max} = 1$ deg and reduced frequency $\omega* = \omega\ c/U_\infty = 0.20$ (related to wing chord). Numerical simulations are performed with the 1-equation S-A model,

the central differencing spatial solver and the following temporal resolution: 500 physical time-steps per oscillation and 40 pseudo-physical time-steps (iterations) per every physical time-step. In order to ensure a converged periodic solution alltogether 5 periods are calculated, resulting in total 2500 physical time-steps. Every period requires about 68 CPU hours on a cluster of 16 Intel P4 2.0 GHz processors.

When the unsteady aerodynamic response (unsteady pressure perturbations) is transformed to the Fourier space, the results are expressed as magnitude and phase shift for the first and second harmonic components of pressure perturbation. Figure 7 depicts the results for three different span-wise positions: the wing cut-plane at 20% span (flow free of WNP channel effects, Figure 7a), the wing cut-plane at 47% span (slice through the WNP channel, Figure 7b) and the nacelle upper cut-plane inclined at 26 deg (in the channel, Figure 7c). For every cut-plane the lower right graph in each figure shows the unsteady variation of pressure distributions during one oscillation period. From the phase shift graphs it can be seen that the variation of Cp is generally not in phase with the motion (incidence angle) of the model, i.e., a significant phase shift between the structural motion and the aerodynamic response can be observed, together with a distinct non-linear nature of the surface pressure fluctuation (relatively high values of the second harmonics).

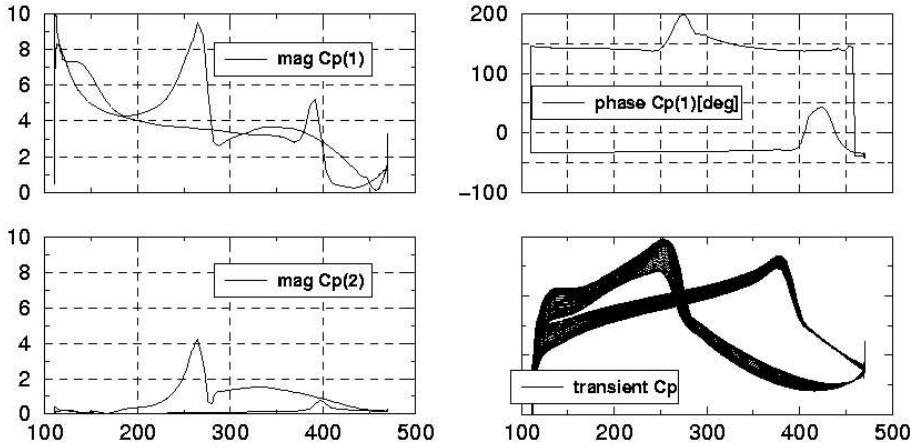

Figure 7a: Magnitude and phase of unsteady pressure (1st and 2nd harmonics) for the Navier-Stokes simulation of forced pitching rotation. Results for the cut-plane at 20% wing span. Magnitude nondimensionalised with the amplitude of oscillation.

At 20% wing span (Figure 7a) shock waves are present on both upper and lower wing surface. On the upper surface, the shock is located close to the trailing edge and is of medium strength. The motion of this shock is nearly harmonical, the fact highlighted by almost zero value for the second harmonic pressure component. Shock on the lower surface is stronger (higher magnitude) and its motion amplitude is larger than on the upper surface (5% and 2% wing chord for the lower and upper surface shock respectively). Correspondingly, the pressure signals are significantly nonlinear, as shown by the larger value of second harmonic for the pressure at shock location and downstream of the shock. On the upper surface the phase is negative (approximately -30 deg) everywhere except in a narrow window downstream of the shock, indicating the pressure phase delay, i.e., the lagging of the unsteady pressure behind the geometry pitching incidence (maximum suction level is reached after the geometry passed the maximum incidence). On the lower surface the phase shift angle is defined with the opposite sign from that on the upper surface, i.e., for the limitting case of zero reduced frequency the maximum pressure is

reached at the minimum incidence (implicit phase delay of 180 deg for a quasi-steady flow). Therefore, the calculated phase angle of approximately 140 deg corresponds to the actual phase angle of about $140 - 180 = -40$ deg, meaning that the phase of pressure perturbation on the lower surface is also delayed against the incidence angle rotation (pressure trailing the incidence).

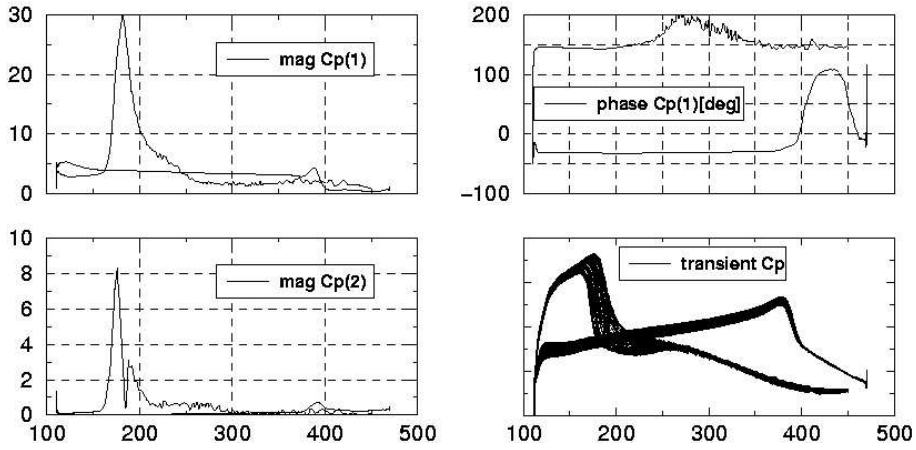

Figure 7b: Magnitude and phase of unsteady pressure for the cut-plane at 47% wing span.

For the second wing cut-plane (at 47% span, Figure 7b) the unsteady pressure perturbation appears to be similar to the above described results. The noticeable differences are much larger pressure peaks (in both the first and the second harmonics) on the lower wing surface which are the result of stronger shock due to the channel effect. Both harmonics exhibit a wavy behaviour which is probably the result of the moving shock-induced flow separation point. The values on the upper wing surface do not differ much from those at 20% span with the only exception that the phase delay angle in the region of shock motion is larger. This confirms the assumption that the upper surface pressure is only marginally affected by the channel flow (nearly constant surface pressure perturbation).

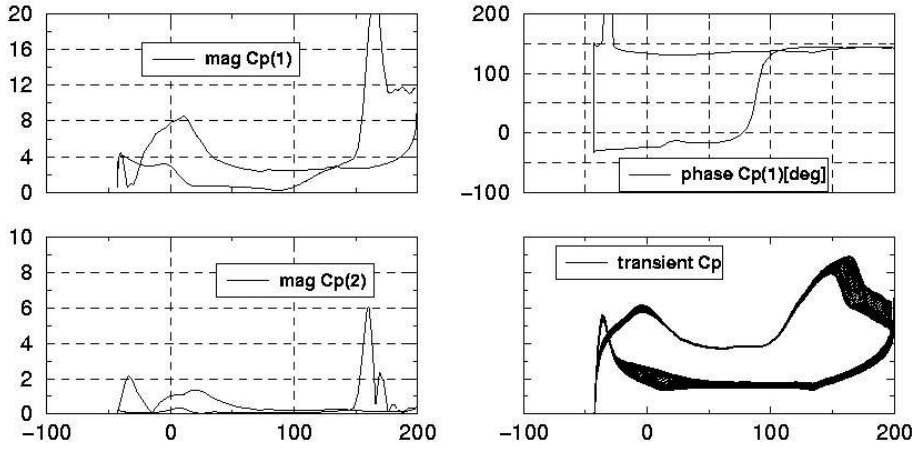

Figure 7c: Magnitude and phase of unsteady pressure for the nacelle cut-plane inclined at 26 deg (only the upper part of nacelle shown).

Results on the nacelle differ from those on the wing surface. Figure 7c shows the results for the third cut representing the lower boundary of the channel. It can be seen that a strong shock on the nacelle outer surface causes the flow separation which extends to the

trailing edge. Significant pressure fluctuations are present in both regions, at the shock location and at the trailing edge, and this is reflected in strong pressure peaks for both first and second harmonics. The magnitude of pressure perturbation remains high all the way to the trailing edge indicating strong unsteady phenomena with the intermittent separation and re-attachment of boundary layer downstream of shock. In the front part of the nacelle cut-plane (up to $x = 80$ cm) a relatively small pressure phase lag is observed (approximately -20 deg) on the nacelle outer skin. Upon entering the shock region the phase shift angle jumps to +140 deg, indicating the large advancement of the pressure phase (pressure perturbation leading the incidence angle). This value is kept all the way to the trailing edge, indicating that shock motion, separation and re-attachment phenomena are nearly in anti-phase with the pitching of the model.

The role of unsteady separation is further demonstrated in Figure 8, which shows the effect of a dynamic shock/boundary-layer interaction and the resulting intermittent local flow separation on the zones of supersonic flow for the 47% span cut-plane. These phenomena have been recognized to play a crucial role in the aerodynamic excitation of the WNP aeroelastic system.

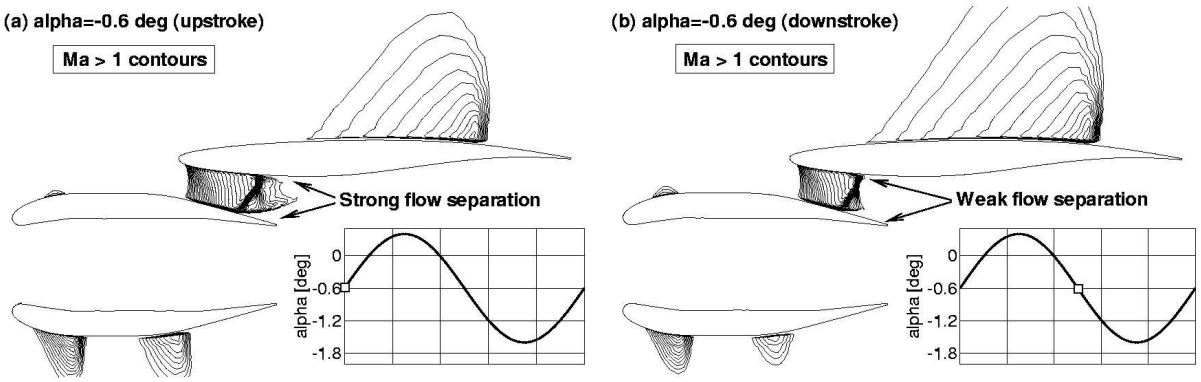

Figure 8: Two snapshots taken during a cycle of pitching oscillation: upstroke (nose-up) and downstroke (nose-down) motion through the mean incidence position.

6 AERODYNAMICS EXCITATION WITH STATIONARY GEOMETRY

Due to the strong interaction between a shock wave and a boundary layer, and the resulting shock-induced flow separation, the unsteady flow phenomena can occur in the WNP region even with a stationary geometry. The self-sustained shock oscillation (shock-buffet) may induce large fluctuation of aerodynamic loads and in that way impose a flight-envelope boundary (limiting factor in a pure aerodynamic sense). Furthermore, since the shock oscillation frequency can be close to the flutter frequency the shock-buffet can excite structural vibrations and therefore represents a limit in an aeroelastic sense. In general, shock-buffet is a large-scale flow-induced shock motion that involves alternating separation and reattachment of the boundary layer. There have been numerous, mainly experimental, studies in the last five decades dealing with shock-buffet on aerofoils and wings [8,10], whereas the recent DNW-TWG measurements with the stationary WIONA geometry [7] hinted at the existence of a natural aerodynamic frequency (shock-buffet) in the WNP interference region. The measured unsteady surface pressure signals from the interference region show a distinct peak of the signal at reduced frequency value of $\omega* = \omega\ c/U_\infty = 2.5$ (c being the wing chord).

In order to validate the prediction capabilities of the Tau flow solver, a thorough analysis of shock/boundary-layer interaction and shock-buffet has been performed using different aerofoil geometries [9]. The onset of shock-buffet was taken as the first incidence angle at which time-accurate calculations returned persistent lift oscillations with the amplitude at least two orders of magnitude larger than any oscillations due to numerical instabilities. Validation of shock-buffet results for 2 symmetrical and one supercritical aerofoil showed that shock oscillations occur only after the flow separation covered the complete rear part of a profile in that way causing the abrupt trailing edge pressure divergence and, subsequently, the fluctuation of overall circulation and global aerodynamic loads. It has been shown that the appropriate choice of modelling parameters for shock-buffet URANS simulations depends on the aerofoil geometry. The 2-equation turbulence model is more successful than the 1-equation model in predicting the shock-buffet phenomena on thin aerofoils (maximum thickness below 12% chord, Figure 9 left). For thicker aerofoils, on the other hand, the 1-equation S-A model gives the buffet onset boundary closer to the experimental data (Figure 9 right). Regarding the underlying physical mechanism of buffet phenomena, the analysis [9] showed that relatively high incidence angles ($\alpha > 4$ deg) are necessary to provoke the onset of shock-buffet on thin aerofoils. With increasing thickness the buffet onset shifts toward lower α-values and, in the case of a 17% thick supercritical aerofoil, buffet can occur even at small negative incidence angles.

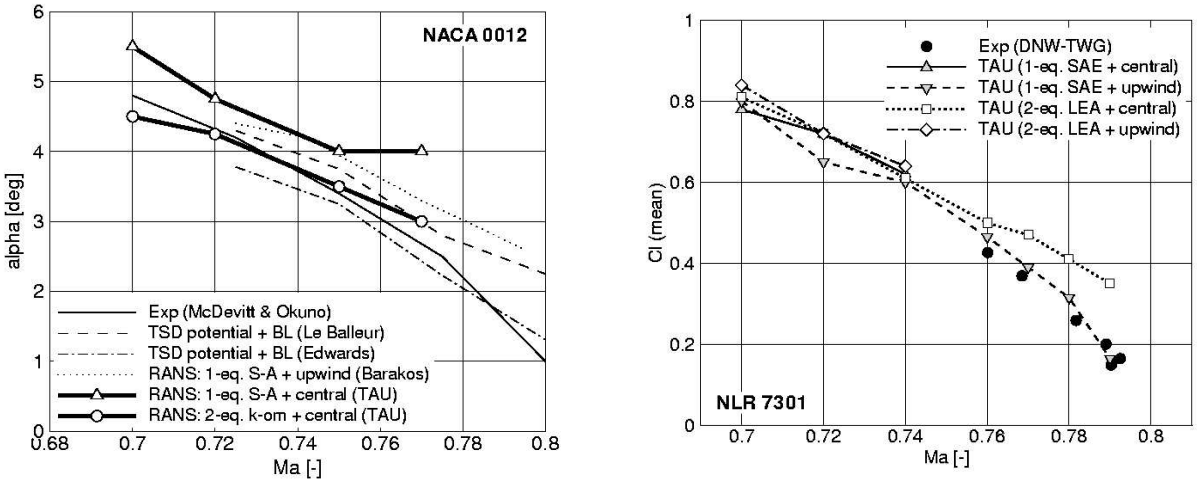

Figure 9: Calculated buffet onset boundaries for two aerofoils. Results obtained with the Tau code compared to the experimental and numerical data from literature (for more details see [9]).

The following modelling parameters are used for the time-accurate calculations with the stationary WIONA geometry: 2-equation LEA turbulence model combined with the central differencing solver and dual-time-stepping with 100 inner-iterations and 3-level multigridding within every physical time-step. The size of physical time-step for simulation is chosen such to enable fine enough temporal resolution of the high buffet reduced frequency found in the experiment: $\Delta t \approx 10^{-5}$ s. For the expected reduced frequency ($\omega* \approx 2.5$) this value gives the resolution of about 250 time-steps per period of shock oscillations. For the buffet simulation a following test case is chosen: $Ma = 0.80$, $Re = 2.3$ million and $\alpha = 0$ deg.

In Figure 10 left, which shows distributions of the instantaneous pressure coefficient for two cut-planes passing through the channel region, the WNP shock wave oscillation and the fluctuation of pressure levels downstream of shock can be seen. Two mechanisms required for the onset of buffet are present in the channel flow: the intermittent shock-induced separation of boundary layer (both on wing and nacelle) and the divergence of the trailing edge pressure (on the upper side of nacelle). The time evolution of the integral lift coefficient for the complete geometry is shown in the right part of Figure 10. The spectral density analysis of the signal shows a distinct peak at approximatelly 230 Hz, which gives a reduced frequency value $\omega* \approx 2.0$ which only roughly corresponds to the frequency found in experiment. The time evolutions of the calculated pressure signals recorded at two characteristic surface points from the channel region are also shown in Figure 10.

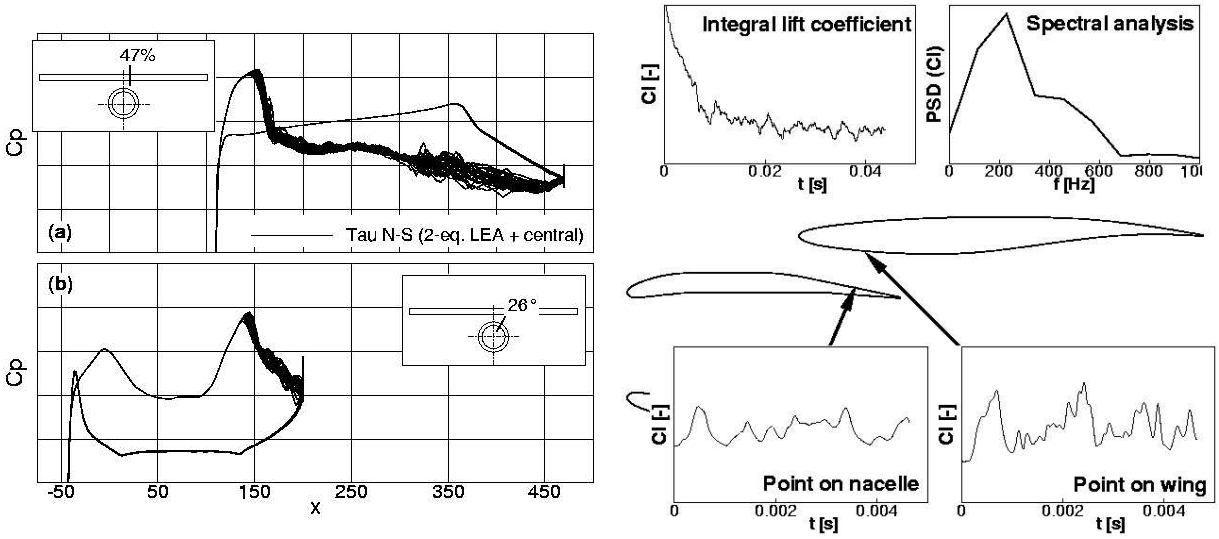

Figure 10: Results of shock-buffet calculation (time-accurate simulation with stationary geometry) for the WIONA model. Left: evolution of instantaneous pressure coefficient at two span-wise cut-planes. Right: evolution of integral lift coefficient and PSD distribution (top), evolution of pressure signals for two points from the WNP region (bottom).

7 CONCLUSIONS

Computational investigation of steady and unsteady aerodynamic flow phenomena has been performed for a generic wing-nacelle-pylon WIONA configuration. In the design phase of WIONA geometry the inviscid (Euler) computations have been employed to test the influence of various geometric parameters and to define the final geometry of WIONA configuration. The steady viscous (Navier-Stokes) solutions show a strong influence of interference effects on steady and unsteady aerodynamic loads in the wing-nacelle-pylon region. The major interference effects are: λ-shock system, shock-induced flow separation, development of recirculation bubbles and boundary layer re-attachment. These results are confirmed by the recent steady wind-tunnel measurements performed at DLR in Goettingen.

The viscous simulation results for the pitching WIONA geometry show the existence of strong non-linear interference effects and the presence of intermittent shock-induced flow separation in the WNP channel. The phase shifts resulting from the interaction of these phenomena could play an important role for the aeroelastic behaviour of the complete

aircraft. Furthermore, all current unsteady numerical results need validation by unsteady wind tunnel test results which will be available in 2006. Finally, the unsteady interference effects could be present also with the stationary geometry, as confirmed by the steady wind-tunnel measurements showing the existence of natural aerodynamic oscillations in the WNP region. The numerical investigation showed the existence of high-frequent shock oscillation but further simulations are needed before the existence of self-sustained periodic shock-buffet oscillations is confirmed.

ACKNOWLEDGMENTS

The current work has been perfromed within the ongoing DLR project $HighPerFlex$. The experimental results have been obtained in the DLR-ONERA project $WIONA$.

REFERENCES

[1] Zingel, H., *Measurements of steady and unsteady airloads on a stiffness scaled model of modern transport aircraft wing*, Proceedings of Int. Forum on Aeroelasticity and Structural Dynamics, DGLR 91-06, Germany, 1991, pages 120-131

[2] Försching, H., *New Ultra-High Capacity Airscraft (UHCA): Challenges and problems from an aeroelastic point of view*, ZFW 18 (1994), pp 219-231

[3] Gerhold, T., et al., *Tau-Code User Guide, Revision: 1.24, April 05, 2004*, DLR, Germany (http://www.taurus.dlr.de/taurus_main.htm)

[4] Soda, A., and Tefy, T., *Numerical Investigation of Wing-Nacelle Interference Effects at Transonic Flow Conditions for a Generic Transport Aircraft Configuration*, New Results in Numerical and Experimental Fluid Mechanics IV (Notes on Numerical Fluid Mechanics and Multidisciplinary Design - Volume 87), Editors: Breitsamter, Laschka, Heinemann and Hilbig, Springer, Germany, 2004

[5] McMorris, H., *Centaur Online User's Manual - Centaur v5.0*, USA, 2003 (http://www.centaursoft.com)

[6] Brodersen, O., and Rossow, C.C.,*Calculation of Interference Phenomena For a Transport Aircraft Configuration Considering Viscous Effects*, 1993 European Forum: Recent Development and Applications in Aeronautical CFD, Bristol, UK, 1993

[7] Dietz, G., et al., *DNW-TWG WIONA Experiment*, DLR Göttingen, Germany, 2003 (private communication)

[8] Finke, K.,*Stoßschwingungen in schallnahen Strömungen*, VDI-Forschungsheft 580, Germany, 1977

[9] Soda, A., and Verdon, N., *Investigation of Influence of Different Modelling Parameters on Calculation of Transonic Buffet Phenomena*, presented at the 14th STAB/DGLR Symposium in Bremen, Germany, 2004 (to be published in conference proceedings in 2005)

[10] Lee, B. H. K., *Oscillatory Shock Motion Caused by Transonic Shock Boundary-Layer Interaction*, AIAA Journal, Vol. 28, No. 5, May 1990, pages 942-944